

## Control of direct band gap emission of bulk germanium by mechanical tensile strain

M. El Kurdi,<sup>a)</sup> H. Bertin, E. Martincic, M. de Kersauson, G. Fishman, S. Sauvage, A. Bosseboeuf, and P. Boucaud<sup>a)</sup>

*Institut d'Electronique Fondamentale, CNRS-Univ Paris-Sud 11, Bâtiment 220, 91405 Orsay, France*

(Received 10 November 2009; accepted 28 December 2009; published online 28 January 2010)

We show that the recombination energy of the direct band gap photoluminescence (PL) of germanium can be controlled by an external mechanical stress. The stress is provided by an apparatus commonly used for bulge or blister test. An energy redshift up to 60 meV is demonstrated for the room temperature PL of a thin germanium membrane (125 nm wavelength shift from 1535 to 1660 nm). This PL shift is correlated with the in-plane tensile strain generated in the film. A biaxial tensile strain larger than 0.6% is achieved by this method. This mechanical strain allows to approach the direct band gap condition for germanium which is of tremendous importance to achieve lasing with this material. © 2010 American Institute of Physics. [doi:10.1063/1.3297883]

Germanium is attracting a considerable interest due to the possibility to achieve laser emission with this material on a silicon platform. Optical gain has been recently reported in a thin germanium film deposited on a silicon wafer.<sup>1</sup> Two main ingredients are at the origin of the enhancement of the optical recombination properties of germanium: *n*-type doping and tensile strain. *n*-type doping allows to fill with carriers the indirect *L* valley and increase the number of carriers transferred into the  $\Gamma$  valley where they can recombine efficiently. The enhancement by *n*-doping of the direct band gap room temperature photoluminescence (PL) of germanium has been demonstrated for germanium on silicon<sup>2</sup> and for germanium-on-insulator layers.<sup>3</sup> The second main ingredient to tailor the germanium optical properties is the in-plane tensile strain. Due to the difference of deformation potential parameters between the  $\Gamma$  and *L* valleys, a biaxial tensile strain leads to a stronger dependence with strain of the energy position of the  $\Gamma$  valley as compared to the *L* valley. It has been theoretically shown that germanium can even become a direct band gap material for a 2% tensile strain.<sup>4,5</sup> Strong optical gain in tensilely strained germanium has been theoretically predicted either using effective mass approaches<sup>6-8</sup> or 30 band  $\mathbf{k}\cdot\mathbf{p}$  formalism.<sup>9</sup> The application of a tensile strain can be obtained by several techniques. A small tensile strain of 0.25% can be obtained by directly depositing relaxed germanium on silicon and taking advantage of the difference of thermal mismatch coefficients between germanium and silicon.<sup>10</sup> Tensilely-strained germanium can also be obtained by growing germanium on materials with a larger lattice parameter like InGaAs buffers.<sup>11</sup> A third option is to apply a mechanical external tensile stress to generate the required strain. This approach offers the advantage to control the amplitude of the deformation and consequently the possibility to tailor the optical properties *ex situ*. Micromechanical strain engineering has been theoretically considered in Ref. 8. In order to present an interest in the framework of optical gain studies on germanium, the applied tensile strain needs to be large enough, i.e., a fraction of percent, in order to have a significant impact on

the *L*- $\Gamma$  valley splitting and on the degeneracy lifting of the valence band.

In this letter, we report on the external control of the optical properties of germanium through a mechanical deformation. The mechanical deformation is provided by a bulge/blister test apparatus normally used to characterize mechanical properties and adhesion of thin films. A biaxial tensile strain larger than 0.6% has been achieved in a thin germanium membrane. The strain is measured through the vertical displacement of the germanium membrane combined with the modeling of the strain profile. This strain leads to a significant change of the room temperature direct band gap recombination of germanium. A spectral shift as large as 60 meV (125 nm) is observed at room temperature on the PL spectra. We show that in this regime the PL is still dominated by the recombination with the heavy holes. The wavelength shift is correlated with the predicted band gap shift as obtained from a 30 band  $\mathbf{k}\cdot\mathbf{p}$  formalism.<sup>12-15</sup> An excellent agreement is obtained between the experimental band gap shift and the theoretical one.

The principle of operation of the bulge test is shown in Fig. 1. A germanium membrane is glued on a metal piece with a drilled circular aperture. The germanium membrane was obtained after chemical etching of a bulk Ge substrate

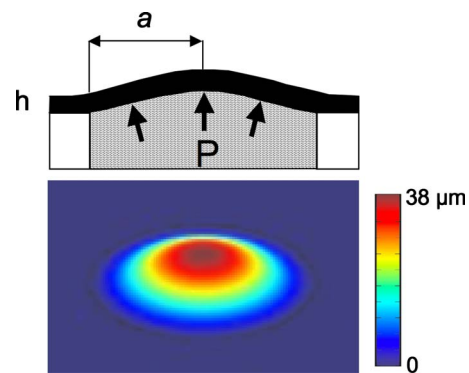


FIG. 1. (Color online) Top: schematic view of the bulge test. The radius  $a$  of the membrane and the thickness  $h$  of the sample are indicated. The liquid is illustrated by the gray area. Bottom: calculated deformed shape of a 28  $\mu\text{m}$  thick germanium membrane strained by a 2.5 MPa load pressure. The vertical scale varies from 0 to 38  $\mu\text{m}$ . The diameter of the blister is 1.45 mm.

<sup>a)</sup>Electronic addresses: moustafa.el-kurdi@ief.u-psud.fr and philippe.boucaud@ief.u-psud.fr.

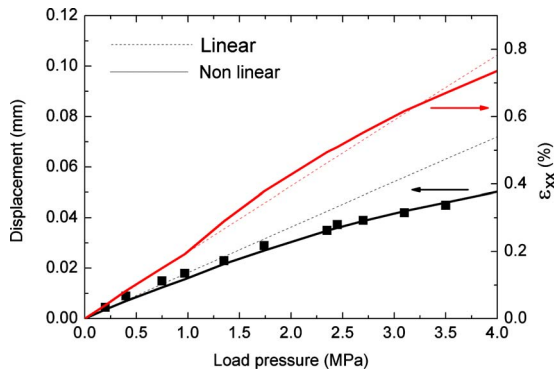


FIG. 2. (Color online) Vertical displacement at the center (left scale) as a function of the load pressure. The squares correspond to the experimental points. The dashed lines correspond to the modeling assuming a purely elastic membrane (linear solver). The full lines correspond to the modeling accounting for the geometry and using a nonlinear stress-strain behavior (nonlinear solver). The right scale corresponds to the calculated in-plane biaxial strain ( $\epsilon_{xx}=\epsilon_{yy}$ ) in the top of the membrane using the linear and the nonlinear models.

using a  $\text{HF}-\text{H}_2\text{O}_2-\text{H}_2\text{O}$  (1-1-1) solution. A uniform water pressure can be applied through the hole of the sample holder to the back side of the Ge membrane by a manual piston or a syringe pump.<sup>16,17</sup> The pressure is measured by a diaphragm pressure sensor. The applied pressure is eventually limited by the debonding of the sample from the metallic support or by sample breaking. The vertical displacement at the center is measured *in situ* by focus deflection with a micro-PL set-up by using the reflection of the optical pump. While the pressure is applied, the PL of the germanium film is measured at room temperature using an argon ion laser as the excitation source. The PL is detected with a liquid-nitrogen cooled germanium photodetector and the spectra have been normalized by the photodetector response. Figure 1 also shows the calculated deformed shape of a germanium membrane by applying a 2.5 MPa pressure. The calculation was performed by using a finite element solver. The displacement is maximum at the center of the pressurized membrane. Knowing the thickness of the membrane, its radius, its center deflection, we can deduce the in-plane strain imposed on the material as a function of the external pressure. The calculation indicates that the strain in the membrane is nonuniform with a biaxial in-plane tensile strain in the top center area and a uniaxial compressive strain at the clamped edges of the membrane. The latter can be significantly larger than the one at the center.

Figure 2 shows the measured vertical displacement at the center of the membrane as a function of the load pressure. The film has a thickness of 28  $\mu\text{m}$  and the vertical displacement can be larger than its thickness. This measurement is compared with the calculated displacement versus load pressure as obtained with a finite element solver. The diameter of the membrane is 1.45 mm. The bulk germanium parameters have been used in the calculation: average Young's modulus  $E=116$  GPa, Poisson ration  $\nu=0.26$ .<sup>18</sup> For weak strains, a standard deformation calculation shows that the vertical displacement  $y$  is equal to  $3(1-\nu^2)Pa^4/16Eh^3$  where  $a$  is the radius of the free surface,  $h$  the thickness of the film, and  $P$  the applied pressure while the in-plane biaxial strain at the center of the membrane is equal to  $3(1-\nu^2)h^2P/8Ea^2$ .<sup>19</sup> These formula indicate that the deformation and the displacement are very sensitive to the radius and to the thick-

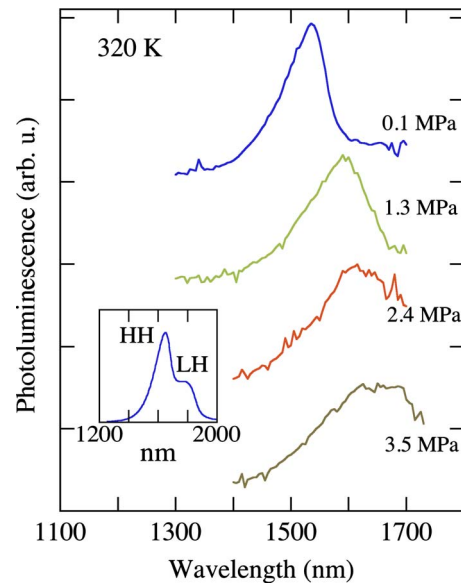


FIG. 3. (Color online) Room temperature PL spectra of the germanium membrane for different load pressures indicated on the right hand side of the figure. The curves have been offset for clarity. The inset shows the calculated recombination spectrum under a 0.7% strain, highlighting the contribution of heavy holes and light holes. The signal-to-noise ratio is smaller at large load pressures because of the detector cutoff.

ness of the membrane. For large strains, the calculation of the vertical displacement as obtained from the finite element solver accounts for the cap geometry, leading to a nonlinear dependence of the vertical displacement as a function of load pressure. The nonlinearities of the stress-strain behavior of the material are also taken into account through the elastoplastic deformation. The accounting of these nonlinearities is justified by the fact that the high pressure measurements are close to the sample fracture. The dashed lines in Fig. 2 correspond to the calculation with a linear dependence versus pressure while the full lines correspond to the results obtained by simulation with the nonlinear solver. A good agreement is obtained between the measurement of the vertical displacement and the calculation using the nonlinear model. As mentioned above, one can also deduce from the calculation the in-plane tensile strain in the top region of the membrane. The calculated in-plane tensile strain is shown in Fig. 2 (right scale) as a function of the load pressure. As seen, a biaxial tensile strain larger than 0.6% is reached for a load pressure of 3.5 MPa.

Figure 3 shows the room temperature PL spectra of germanium for different load pressures. The PL significantly shifts toward long wavelength as the pressure is increased. The redshift reaches the value of 60 meV (125 nm) for a load pressure of 3.5 MPa. In-plane tensile strain has two main effects on the germanium band structure. It decreases the energy of the  $\Gamma$  valley and lifts the degeneracy between heavy holes and light holes in the valence band. The extremum of the valence band is thus theoretically given by the light hole band. However, heavy hole and light hole bands have different effective masses of density of states and different dipole matrix elements. Even if the extremum is given by the light hole band, the calculation of the recombination spectrum shows that the PL is dominated by the recombination with heavy holes for moderate tensile strains. The inset of Fig. 3 shows a calculated recombination spectrum for a

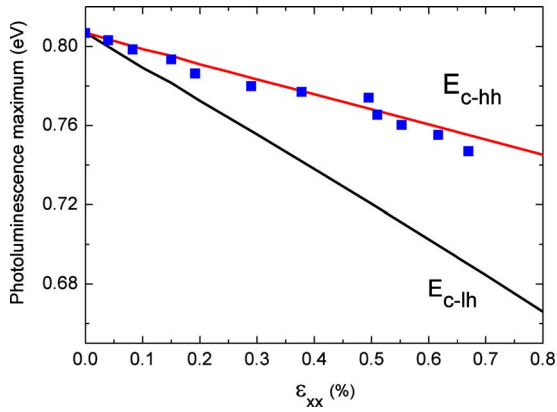


FIG. 4. (Color online) Dependence of the PL peak maximum as a function of the in-plane biaxial tensile strain (squares). The PL peak maximum is obtained from measurements as shown in Fig. 3. The in-plane strain is obtained by the calculation shown in Fig. 2 based on the measurement of the vertical displacement. The full lines correspond to the dependence of the PL maximum between the  $\Gamma$  valley and the heavy holes ( $E_{c-hh}$ ) and light hole bands ( $E_{c-lh}$ ) as obtained from a 30 band  $\mathbf{k}\cdot\mathbf{p}$  formalism.

tensile strain of 0.7% where the contribution of light hole bands and heavy hole bands are distinguished. As seen, the PL is still dominated by the recombination with the heavy holes. It implies that the wavelength shift observed in Fig. 3 is related to the recombination between the  $\Gamma$  valley and the heavy hole band. This point is of importance since the dependence of the band gap implying heavy holes and light holes is significantly different. We have also checked that the wavelength shift is nonuniform along a diameter of the membrane as predicted by the calculation presented in Fig. 1. The wavelength shift decreases as we move away from the center of the hole and even changes its sign at the edge where a blueshift of the PL is observed.

Figure 4 shows the dependence of the PL maximum as a function of the in-plane biaxial strain. A quasi-linear dependence is reported. This dependence is compared with the calculated dependence of the PL maximum involving the  $\Gamma$  band and the heavy or light hole bands as deduced from the calculated band structure using a 30 band  $\mathbf{k}\cdot\mathbf{p}$  formalism.<sup>9</sup> This PL energy variation results from the dependence of the energy positions of the bands as a function of hydrostatic and uniaxial strains. The temperature of the sample deduced from the energy position of the PL maximum at zero applied pressure and which accounts for the heating due to the optical pump is 320 K. The PL shift for the  $\Gamma$ -heavy hole band can be expressed by the effective following relation obtained from the 30 band  $\mathbf{k}\cdot\mathbf{p}$  formalism  $\Delta E_{PL} = -7.8\varepsilon_{\parallel}$  (eV) where  $\varepsilon_{\parallel} = \varepsilon_{xx} = \varepsilon_{yy}$  is the biaxial in-plane strain. As seen in Fig. 4, the slope is much larger for the light holes. A very good agreement is obtained between the experimental dependence of the PL energy and the calculated one. It indicates that the spectral shift can unambiguously be attributed to the in-plane

strain of the germanium film and to the recombination between  $\Gamma$  and heavy hole band. It also demonstrates that an external mechanical stress is very effective to tailor the optical properties of germanium, in agreement with previous theoretical studies. Meanwhile, the possibility to control tensile strain in germanium with a large amplitude represents a significant step to achieve large optical gains in this material and opens promising perspectives for light-emitting devices and high performance lasers using germanium on a silicon platform.<sup>20-22</sup> For that purpose, the resonators could be provided by standard waveguides with cleaved facets or photonic crystal cavities.<sup>23,24</sup>

This work was partly supported by the French Ministry of Industry under Nano2012 convention and by “Triangle de la Physique.”

- <sup>1</sup>J. Liu, X. Sun, L. C. Kimerling, and J. Michel, *Opt. Lett.* **34**, 1738 (2009).
- <sup>2</sup>X. Sun, J. Liu, L. C. Kimerling, and J. Michel, *Appl. Phys. Lett.* **95**, 011911 (2009).
- <sup>3</sup>M. El Kurdi, T. Kociniewski, T.-P. Ngo, J. Boulmer, D. Debarre, P. Boucaud, J. F. Damlencourt, O. Kermaerrec, and D. Bensahel, *Appl. Phys. Lett.* **94**, 191107 (2009).
- <sup>4</sup>R. Soref, J. Kouvetakis, and J. Menéndez, *MRS Symposia Proceedings No. 958* (Materials Research Society, Pittsburgh, 2007), p. 13.
- <sup>5</sup>J. Menéndez and J. Kouvetakis, *Appl. Phys. Lett.* **85**, 1175 (2004).
- <sup>6</sup>J. Liu, X. Sun, D. Pan, X. Wang, L. C. Kimerling, T. L. Koch, and J. Michel, *Opt. Express* **15**, 11272 (2007).
- <sup>7</sup>S.-W. Chang and S. L. Chuang, *IEEE J. Quantum Electron.* **43**, 249 (2007).
- <sup>8</sup>P. H. Lim, S. Park, Y. Ishikawa, and K. Wada, *Opt. Express* **17**, 16358 (2009).
- <sup>9</sup>M. El Kurdi, G. Fishman, S. Sauvage, and P. Boucaud, *J. Appl. Phys.* **107**, 013710 (2010).
- <sup>10</sup>Y. Ishikawa, K. Wada, D. D. Cannon, J. Liu, H.-C. Luan, and L. C. Kimerling, *Appl. Phys. Lett.* **82**, 2044 (2003).
- <sup>11</sup>Y. Bai, K. E. Lee, C. Cheng, M. L. Lee, and E. A. Fitzgerald, *J. Appl. Phys.* **104**, 084518 (2008).
- <sup>12</sup>S. Richard, F. Aniel, and G. Fishman, *Phys. Rev. B* **70**, 235204 (2004).
- <sup>13</sup>S. Richard, F. Aniel, and G. Fishman, *Phys. Rev. B* **72**, 245316 (2005).
- <sup>14</sup>M. El Kurdi, S. Sauvage, G. Fishman, and P. Boucaud, *Phys. Rev. B* **73**, 195327 (2006).
- <sup>15</sup>M. El Kurdi, G. Fishman, S. Sauvage, and P. Boucaud, *Phys. Rev. B* **68**, 165333 (2003).
- <sup>16</sup>M. K. Small and W. D. Nix, *J. Mater. Res.* **7**, 1553 (1992).
- <sup>17</sup>R. Yahiaoui, K. Daniae, S. Petitgrand, and A. Bosseboeuf, *Proc. SPIE* **4400**, 160 (2001).
- <sup>18</sup>J. J. Wortman and R. A. Evans, *J. Appl. Phys.* **36**, 153 (1965).
- <sup>19</sup>S. Timoshenko and S. Woinowsky-Krieger, *Theory of Plates and Shells*, 2nd ed. (McGraw-Hill, New York, 1959).
- <sup>20</sup>T. Brunhes, P. Boucaud, S. Sauvage, F. Aniel, J. M. Lourtioz, C. Hernandez, Y. Campidelli, O. Kermaerrec, D. Bensahel, G. Faini, and I. Sagnes, *Appl. Phys. Lett.* **77**, 1822 (2000).
- <sup>21</sup>S.-L. Cheng, J. Lu, G. Shambat, H.-Y. Yu, K. Saraswat, J. Vuckovic, and Y. Nishi, *Opt. Express* **17**, 10019 (2009).
- <sup>22</sup>X. Sun, J. Liu, L. C. Kimerling, and J. Michel, *Opt. Lett.* **34**, 1198 (2009).
- <sup>23</sup>M. El Kurdi, S. David, X. Checoury, G. Fishman, P. Boucaud, O. Kermaerrec, D. Bensahel, and B. Ghyselen, *Opt. Commun.* **281**, 846 (2008).
- <sup>24</sup>T.-P. Ngo, M. El Kurdi, X. Checoury, P. Boucaud, J. F. Damlencourt, O. Kermaerrec, and D. Bensahel, *Appl. Phys. Lett.* **93**, 241112 (2008).